Zirconia-supported hybrid organosilica microporous membranes for CO_2 separation and pervaporation

Tim Van Gestel [1,*], Frans Velterop [2], Wilhelm A. Meulenberg [1,3]

Abstract

Hybrid organosilica membranes have great potential for realizing high-flux, high-selectivity gas separation and pervaporation. Current membranes, however, have one major problem: the intermediate layers between the selective layer and the porous support are made of unstable γ-alumina. In this article, a strongly improved membrane set-up based on mesoporous stabilized zirconia (8YSZ) intermediate layers is reported. This novel membrane showed selectivities in the range of 20–30 for different CO_2/N_2 mixtures and accompanying CO_2 permeances of 1.5–4 $m^3/(m^2.h.bar)$. In pervaporation tests with water/isopropanol and water/butanol mixtures (5 wt.% water), the membrane selectively separated water (separation factor ~150 – 600) and an excellent flux of ~5 kg $m^{-2}h^{-1}$ was achieved at 70°C. These results represent an important step towards the industrial application of hybrid silica membranes in applications such as pervaporation as well as the selective removal of CO_2. The analysis also shows for the first time that effective gas separation and pervaporation is realized when γ-alumina is substituted for another, more stable membrane material.

[1] Forschungszentrum Jülich GmbH, Institute of Energy and Climate Research 1 (IEK-1), D-52425 Jülich, Germany
[2] PERVATECH BV, Heliumstraat 11, 7463 PL Rijssen, the Netherlands
[3] University of Twente, Faculty of Science and Technology, P.O. Box 217, 7500 AE Enschede, the Netherlands
[*] Corresponding author; E-mail: t.van.gestel@fz-juelich.de

1. Introduction

In the past few decades, numerous attempts have been made to develop microporous amorphous silica membranes for the separation of gas and vapour mixtures. Some of these membranes are very effective molecular sieves and can directly separate molecules with a kinetic diameter of ~0.3 nm, for instance He (0.26 nm), H_2 (0.29 nm) and H_2O (0.26 nm) [1-4]. Moreover, the adsorption behaviour of silica also enables the separation of CO_2 from gas mixtures, even when the pore diameter of the membrane considerably exceeds the kinetic diameter of CO_2 (0.33 nm) [5-7]. As such, silica membranes have long been considered promising candidates for separation and purification technologies, with applications in numerous important fields. However, they suffer from one severe drawback: instability in a water-containing atmosphere, as is often encountered in realistic industrial applications. This instability is believed to be due to the disruption of the –Si–O–Si– bonds, leading to destruction of the microporous silica network and hence of the membrane´s separating ability [8-10]. An interesting strategy to solve this problem was reported in a number of papers by co-workers in ten Elshof´s group at the University of Twente, in cooperation with the Energy Centre Netherlands (ECN) [11-20]. Their work focuses on modifying the instability of the silica network through the incorporation of hydrolytically stable –Si–C–Si– bonds. According to the authors, this provides a higher internal network connectivity, enhanced mechanical and chemical properties, and a lower sensitivity of the silica network bonds to hydrolysis. The resulting membranes were termed hybrid (organo)silica membranes and were later commercialized under the name HybSi® [21].

The preparation of such a hybrid silica membrane is based upon using a bridged bis-silyl compound as the sol-gel precursor. Most studies reported so far have used the ethylene-bridged compound 1,2-bis(triethoxysilyl)-ethane (BTESE) or, alternatively, its methylene-bridged analogue BTESM. Otherwise, the synthesis pathway is the same as for common TEOS-derived amorphous silica membranes [e.g. 22-24]. Carrier structures are generally made from α-alumina powders and may be simple discs or extruded tubular shapes with a graded porous structure which are commercially available for ultrafiltration. Since both the pore size and the surface quality of these macroporous materials is not suitable for supporting a thin-film microporous membrane, they are modified with

mesoporous intermediate membrane layers by dip coating with nanoparticle dispersions. In the published literature, these intermediate layers are almost exclusively made of γ-alumina, derived from a boehmite-polyvinyl alcohol (PVA) sol. Two slightly different synthesis routes can be distinguished for the preparation of the functional hybrid silica top layer. The first route involves synthesis using an equimolar mixture of BTESE and another Si-precursor, e.g. methyl-triethoxysilyl-ethane (MTES). This method was introduced by Ashimah Sah in 2006 [25,26] to make the first hybrid silica membrane ever reported, which was prepared on a disc-shaped (39 mm) γ-alumina mesoporous membrane by dip coating. In gas permeation tests at 200°C, the membrane was selective for the large molecule SF_6, and it also exhibited selective water permeation in pervaporation with a 5 wt.% aqueous solution of n-butanol at 95°C (separation factor ~100). Following this work, Castricum *et al.* reported on a similar tubular membrane 250 mm in length. This showed stable separation selectivity in the dehydration of n-butanol at 150°C for more than 700 days, with an initial water flux >10 kg/m^{2}h, which decreased slowly to 50% of its value after 400 days. At the same time, Castricum also described a second route, using purely BTESE or BTESM to prepare the coating solution. Although the pure BTESE membrane exhibited larger pores than that derived from a mixture with MTES, the separation factor in water/n-butanol pervaporation was found to improve further. Kreiter *et al.* subsequently reported an even higher water flux and separation factor after replacing the ethylene bridge (BTESE) in the membrane by methylene (BTESM). For a more detailed overview of the developments in this field, we recommend the reader to consult the review article by Andre ten Elshof [10]. We also refer here to the studies by Kanezashi *et al.* [27-29], Qi *et al.* [30,31], Tsuru *et al.* [32], Wolf *et al.* [33] and ten Hove *et al.* [34].

Taken together, all the studies performed so far suggest that the application of hybrid silica membranes is feasible in, for instance, affinity-based CO_2 removal and industrial water pervaporation. In addition, studies on doped membranes suggest that they could even be used for size-based H_2 separation. Any large-scale commercial application of either of these new membranes will, however, also require suitable mesoporous intermediate layers to support them. Currently, there is a major problem with hybrid silica membranes since in almost all the functional membranes reported to date they are made of γ-alumina. While γ-alumina membrane layers have several well-known advantageous characteristics (easy and reproducible preparation route, thickness > 1 μm, pores < 5 nm), their stability is unsatisfactory for most practical applications. The main challenge today in the development and commercialization of hybrid silica membranes is therefore to identify a suitable alternative which combines the same features as γ-alumina with significantly improved stability. Intuitively, an obvious candidate would be a mesoporous titania or zirconia membrane. These exhibit much higher chemical stability and are today commercially available from several membrane manufacturers as tight ultrafiltration (UF) membranes [e.g. 35-38]. Also, a few groups have already reported titania and zirconia mesoporous membranes with mean pore sizes of ~5 nm or less [e.g. 39-41]. However, to the best of our knowledge, there are no reports on their implementation in a membrane system with a hybrid silica top layer. Presumably, the main problem faced by all researchers so far has been the difficulty in producing a titania or zirconia membrane with a combination of the same pore size and surface quality as a γ-alumina membrane.

Here, we report for the first time the use of a zirconia membrane as a support for a functional hybrid silica top layer. This membrane is prepared by dip coating either a disc-shaped or tubular α-alumina support in two different zirconia–PVA nanoparticle dispersions, yielding a graded structure with pore diameters of ~5 nm and ~3 nm. This work was inspired by observations made in two earlier investigations. Firstly, the same zirconia membrane was already successfully employed for the fabrication of ultra-thin (5–10 nm) graphene-based thin films. Evaluation of the resulting 8YSZ/graphene composite membranes in gas permeation and pervaporation tests revealed molecular sieving behaviour for the smallest gases He and H_2 and an exceptional water flux and separation selectivity [42]. Secondly, the zirconia membrane consists of stabilized zirconia, in which the crystal structure is made thermally stable by the addition of 8 mol% yttria, and stability test results demonstrated excellent chemical, thermal and even hydrothermal stability under harsh conditions [43]. It is also worth mentioning that the membrane is produced using a simple and scalable synthetic methodology, which enables commercial grade α-alumina supports to be coated in a reproducible way.

In the experimental studies described in this paper, permeation tests with different small gas molecules were conducted to evaluate the separation performance of the novel 8YSZ/hybrid silica membrane. As the initial results

strongly suggested an affinity-based selectivity for CO_2, we continued to measure the performance of the membrane for separating CO_2/N_2 mixtures. The main purpose was to evaluate its applicability for the capture of CO_2 emitted from coal-fired power plants, which is an area of considerable research interest in order to reduce the emission of CO_2 into the atmosphere. Typically, the combustion exhaust gas (flue gas) produced at such a power plant contains 10–15% CO_2 and the rest is mainly N_2. The standard process employed for CO_2 capture is amine absorption, which is energy- and capital-intensive and environmentally hazardous [5-7]. A membrane-based capture process would provide significant advantages, but suitable membranes combining the necessary CO_2 selectivity and permeance while also meeting the stability requirements are not yet available. For example, the currently available commercial polymer membranes do not meet these criteria and the existing sol-gel silica membranes cannot be used due to their instability under humid conditions. Alternative membrane materials that could be used here are zeolites [e.g. 44] and carbon [e.g. 45], provided that they can be produced economically with sufficient areas and selectivity for this large-scale application. In a second study, we measured the performance of the 8YSZ/hybrid silica membrane for separating water/alcohol mixtures, which is an important pervaporation application. It is worth mentioning that water pervaporation has been frequently proposed as the major application of hybrid silica membranes. Obviously, using highly water tolerant and chemically stable 8YSZ intermediate layers has many advantages here, especially when aggressive compounds are present in the feed mixture (e.g. nitric acid, acetic acid). While working on this study, we tested the dehydration of three different alcohols: ethanol, isopropanol and n-butanol.

2. Experimental methods

2.1. Membrane formation

The substrate used for membrane deposition is a single-channel macroporous α-alumina tube (o.d. 10 mm, i.d. 7 mm) obtained from Fraunhofer IKTS Hermsdorf (Germany). It consists of a bulk support with a pore size of ~10 μm and three layers with gradually decreasing pore diameters on the inside; the average pore size of the final layer is ~70 nm. The as-received substrate tube had glass seals of ~12 mm at both ends, which allowed easy handling during the coating processes and convenient sealing in the different permeation cells. Unless otherwise stated, the length of the tube was 250 mm and the effective permeation area 4970 mm^2. In order to study the gas permeation behaviour, preliminary experiments were conducted with membranes prepared on a macroporous α-alumina disc (d. 40 mm, thickness 2 mm) with a similar pore size of ~80 nm (*see also Section 2.3*). The latter was obtained from Pervatech BV (the Netherlands).

The mesoporous 8YSZ intermediate layers were deposited by a special dip-coating method, as described in detail in reference no. 43. Here, the α-alumina substrate tube was not strictly speaking dipped in the 8YSZ sols, but a syphon dip-coating method was employed, producing 8YSZ layers on the inside of the tube. As can be seen in Fig. S1, the coating device is equipped with a holder for the substrate and a holder for a reservoir with the coating liquid. Coating was performed by moving the liquid reservoir upwards, while the substrate remained in the same position. After 30 s, the reservoir was moved downwards again. During this process, the filling and emptying speed of the substrate was 10 mm/s. To obtain the best possible surface properties (low roughness, no or few defects, pore size ~3 nm) two different water- and PVA-based 8YSZ sols with a particle size of ~60 nm and ~30 nm, respectively, were used as coating liquids. The substrate tubes were coated twice under clean room conditions and each coating step was followed by drying in air for 1 h and calcination in air at 500°C for 2 hours (heating and cooling rate 1°C/minute).

Subsequently, a hybrid silica thin film was prepared on top of the final 8YSZ layer using the same syphon dip-coating device (reservoir speed 10 mm/s, holding time 30 s). A suitable coating liquid was obtained in a similar way to that described in the articles on γ-alumina-supported hybrid silica membranes by researchers of the University of Twente. This involved the synthesis of 100 ml of an ethanol-based sol, starting from 16.655 ml 1,2-bis(triethoxysilyl)-ethane (BTESE, Sigma Aldrich), 28.14 ml ethanol (Sigma-Aldrich Chromosolv), 4.57 ml water and 0.63 ml nitric acid (65%). In comparison with the previously described methods, the synthesis procedure was simplified: the precursor was mixed rapidly with water and no cooling with an ice bath was applied. The obtained

mixture was then heated at 60°C for 90 minutes and allowed to cool to room temperature. The resulting transparent hybrid silica sol was then diluted once by adding 50 ml of ethanol. Importantly, this diluted hybrid silica sol needed to be further diluted ten times with ethanol. This appeared to be a crucial processing step, which determined the success or failure of the formation of the 8YSZ-supported membrane. The as-deposited hybrid silica film was air dried for approx. 1 hour and thermally treated at 300°C for 1 hour in vacuum (heating and cooling steps 1°C/minute), using a special furnace (Gero HTK 25 Mo/16-1G) in which a high vacuum was created (~10^{-4}–10^{-5} mbar). In some cases, thermal treatment was also performed at 450°C and, if so, this is explicitly mentioned in the results section. The entire coating-drying-heating process was carried out twice and at this point the membrane was ready for use in characterization tests.

2.2 Structural characterization

To image the different membrane layers, high-resolution FE-SEM pictures were taken with a Zeiss Ultra 55 microscope at 15 kV accelerating voltage. Prior to SEM analysis, the middle part of the membrane tube was smashed with a small hammer, which resulted in small broken fragments with dimensions of a few square millimetres ; one of which was coated with a platinum layer and a piece of copper tape was then attached to create an electrical contact. The Kelvin pore size distribution was determined using the permporometry method. Essentially, this method is based on the use of the Kelvin equation, and therefore it is in principle only applicable for mesoporous membranes [46,47]. However, in practice, it appeared that permporometry is also useful for the qualitative analysis of microporous membranes. For instance, good results were achieved for silica–zirconia [48], titania [49] and also hybrid silica [12,19] membranes. In the present work, measurements were performed using an apparatus designed and built by Fraunhofer IKTS Hermsdorf. This apparatus is equipped with two gas lines with mass flow controllers (MKS PR4000B); one line is used to supply a dry gas fraction to the membrane and the second line passes through a gas saturator. As pores in the range of ~1 nm or smaller were expected, helium and water were selected as the inert carrier gas and condensable vapour, respectively [12,48]. The membrane was placed in a stainless steel 3-port tubular membrane holder and Viton O-rings were attached to the glass seals at both ends. Then, the permeance of dry helium was determined at 25°C and ~0.2 bar using a gas flow meter (Agilent Technologies ADM 2000). Subsequently, the relative humidity of the helium feed gas was increased in 5% steps and the permeance was recorded. This resulted in a graph with the helium permeance as a function of the relative humidity. A permeance vs. Kelvin radius (r_k) plot was calculated with the aid of the modified Kelvin equation: $r_k = - 2\gamma V_m / RT \ln (p/p_0)$, where γ and V_m are the surface tension and molar volume of water, respectively. This plot represents the size distribution of the Kelvin radii of the effective pores of the membrane [46,47]. The pores of the hybrid silica membrane were assumed to be cylindrical. The corresponding pore diameter (d_p) is thus equal to $2r_k + 2t$, where t is the thickness of a monolayer of water, which is adsorbed on the pore wall before capillary condensation takes place. For the sake of simplicity, 0.26 nm (kinetic diameter of water) is used as the t-layer thickness value.

2.3 Gas permeation and separation experiments

Single gas permeation tests were performed using a home-made set-up, equipped with a stainless-steel membrane holder. To obtain the best possible membrane quality for these specific tests, an α-alumina disc with an optimal highly polished surface was used as the substrate, instead of the commercial grade α-alumina tube. In parallel, a conventional γ-alumina/hybrid silica membrane was also prepared on such an α-alumina disc and tested in the same manner as the control sample. The membranes in the module were sealed by compressing a Viton O-ring with a diameter of 20 mm directly on the membrane surface (effective permeation area 314 mm²). The gas permeance was measured in the dead-end mode at a feed pressure of 5 bar for different test gases with increasing kinetic diameter (He (0.26 nm), H_2 (0.289 nm), CO_2 (0.33 nm), N_2 (0.364 nm)). The pressure at the feed side was set and precisely controlled using a Brooks 5866 pressure controller, while the pressure at the retentate side was atmospheric. The gas flow through the membrane was measured by Brooks smart mass flow meters with maximum flow ranges of 200, 40 and 8 ml min^{-1}. To reach the required temperature (20–200°C), the membrane holder was placed inside a laboratory oven (Heraeus T6). These single gas tests were mainly intended to identify possible application fields for the novel membrane. As could be expected for a membrane having pores of ~1 nm, the

permselectivity of H_2 over CO_2 and N_2 was only between low to moderately good. At the same time, a comparatively high CO_2 permeance was measured (~1.5 10^{-7} mol/(m^2.s.Pa)), which was also found to decrease at increasing temperatures, suggesting that adsorption of CO_2 in the pores played an important role. Therefore, further experimental investigations were focused on the separation of CO_2 from a binary gas mixture.

Binary gas permeation experiments were conducted at temperatures of 20–150 °C with a cross-flow permeation set-up, which was also designed and built by Fraunhofer IKTS Hermsdorf. Given the results from single gas tests, CO_2/N_2 mixtures with three different compositions were tested (50, 15 or 10 vol.% CO_2). The membrane sample (250 mm tube) was placed in a 3-port tubular membrane holder, sealed with the aid of Viton O-rings, and the holder was then wrapped with heating tape. A thermocouple was inserted for temperature detection and control. Prior to experimentation, the membrane was heated at 150°C using a N_2 flow rate of 100 ml min^{-1}. After preheating, the N_2 flow was switched off and the CO_2 and N_2 flow were set at the desired flow rate (total flow rate 2000 ml min^{-1}), and a vacuum was maintained on the permeate side (Pfeiffer MVP 015-2). All gas flows were controlled using high-precision MKS flow controllers. An infrared sensor was used to determine the CO_2 concentration in the permeate gas stream in combination with a Mesalabs Defender 530+ gas flow meter. The CO_2 selectivity was expressed as the separation factor, which is defined as the enrichment factor of CO_2 in the permeate compared to the feed composition, $\alpha_{CO2,N2} = (y_{CO2}/y_{N2})/(x_{CO2}/x_{N2})$, where y_{CO2} and y_{N2} are the fractions of CO_2 and N_2 in the permeate, and x_{CO2} and x_{N2} are their corresponding fractions in the feed. In this study, the entire testing protocol was carried out consecutively with four identically prepared membrane samples to check the reproducibility of the membrane manufacturing processes.

2.4 Pervaporation experiments

Pervaporation experiments were performed with a cross-flow test unit at Pervatech BV (the Netherlands). Initially, a series of shorter 105 mm tubes was tested to provide a rapid estimate of the possible performance of the membrane. The feed solution in these quick tests contained 5 wt.% water and 95 wt.% isopropanol (IPA). Testing conditions comprised a temperature of 70°C, vacuum pressure of ~10 mbar, flow of ~300 l/h, and the feed volume was ~2 l. During the tests, the permeate stream was collected by a liquid N_2 trap and the permeate flux was determined by weighing. The water concentration in the permeate and the feed solution was measured with a refractometer and Karl Fischer titration, respectively. The separation factor, $\alpha_{water,alcohol}$, was calculated as follows: $(y_{water}/y_{alcohol})/(x_{water}/x_{alcohol})$, where y and x are the weight fractions of water and alcohol on the permeate and feed side, respectively. For each membrane sample, the pervaporation test was repeated three times to ensure the reliability of the results. It appeared that the membrane was very functional, and therefore an extensive alcohol dehydration study was carried out with four larger 250 mm tubes. This study involved different feed solutions containing 5 wt.% of water and 95 wt.% of ethanol (EtOH), isopropanol (IPA) or n-butanol (n-BuOH), and varying operating temperatures of 70 to 150°C. Also, at the latter higher temperatures, the experiments were performed in the pervaporation mode. When we fill the feed tank with the test solution, we apply 1 bar over-pressure with N_2. Then, we start heating to the desired temperature. When the temperature exceeds the boiling point, pressure will build up, and the liquid remains liquid because of the over-pressure. The higher the temperature, the higher the pressure will be, and the liquid remains liquid.

3. Results

Figure 1 shows SEM images of the cross-section and surface of an 8YSZ/hybrid silica membrane sample. To visualize the distinct membrane layers, we first tested the common in-lens mode and then switched to a back-scattered electron (BSE) detector, as it appeared that this was necessary to obtain suitable images. Indeed, by using conventional SEM – as performed in previous studies on γ-alumina-supported membranes – the different layers of the membrane could be hardly identified (Fig. S2). In contrast, in the BSE mode, the individual layers became clearly visible, because the colour and brightness of the hybrid silica layer (dark grey) differed strongly from the 8YSZ sublayer (bright white) (Fig. 1A). Moreover, BSE images also revealed the asymmetric graded structure of the sublayer, consisting of a thicker (~1 μm) layer with a pore size of ~5-6 nm, to compensate for the roughness

of the substrate tube, and an additional thinner smoother layer with a pore size of ~3-4 nm. As shown in panel B, the hybrid silica top layer is ~150 nm thick, and it is clearly well attached to the final 8YSZ layer. Importantly, substituting the γ-alumina intermediate layers into the novel layers made of 8YSZ did not result in significant changes in the appearance and thickness of the top layer. For comparison, Castricum *et al.* [15] observed a 160-nm-thick hybrid silica layer on top of a ~1-µm-thick γ-alumina layer in their SEM investigations. In the surface views (Figs. 1C and 1D), the 8YSZ layers also appeared to be very uniformly covered by the hybrid silica layer, with no detectable cracks. Close examination of the surface however revealed that the topography of the membrane is quite uneven and contains a few defects, which are marked with black arrows. This is probably due to some localized roughness of the substrate tube, which was transferred to the intermediate layers and, in turn, to the hybrid silica top layer. However, apart from that, we can see that the applied manufacturing processes delivered membrane layers that follow the geometry of the substrate effectively. These SEM results thus provided a first indication that the mesoporous 8YSZ membrane developed in-house is perfectly suited as a sublayer for a high-quality hybrid silica top layer.

The Kelvin pore size distribution was determined by permporometry to discover whether the resulting 8YSZ/hybrid silica membrane also exhibited the desirable fine microporous structure. From the He permeance vs. Kelvin diameter plot (Fig. 2), it can be seen that a large number of the pores became blocked in the range corresponding to a Kelvin diameter < 1 nm. The membrane thus clearly exhibits a microporous character and the sharp decline in permeance tells us that the pore size distribution is quite narrow. The average Kelvin diameter (d_k) of the measured samples, which is defined as the value at which 50% of the initial He permeance was reached, is equal to 0.5–0.7 nm. Taking the t-layer thickness into account, an average pore diameter (d_p) of ~1 nm is therefore obtained. The tail of the permporometry plot indicates, however, that the measured samples also contained a fraction of larger pores with a diameter > 1 nm. The presence of such relatively large pores seems to be a significant drawback for the envisaged applications, e.g. the separation of small gas or vapour molecules. Nonetheless, the results of the novel membrane are in good agreement with previous results for a BTESE-derived membrane deposited on γ-alumina, confirming that the manufacturing processes worked perfectly. For example, Kreiter *et al.* [19] reported the same average Kelvin diameter of ~0.6 nm and mentioned that a significant portion of the overall He permeance was caused by pores larger than 1 nm. It is also worth noting that a set of 6 membrane samples was tested in the present study and the He permeance plots displayed in Figure 2 are nearly the same, thus demonstrating good repeatability for the manufacturing processes. For comparison, the Figure shows also the permporometry plots of the corresponding 8YSZ sublayers, obtained before coating with the hybrid silica top layer, using N_2 as carrier gas. The observed average effective pore diameter (corrected for the t-layer) was ~3-4 nm, and the N_2 permeance became negligibly small in the Kelvin diameter region from 5 nm upwards.

Subsequently, single gas permeation tests were conducted with different gases (He, H_2, CO_2, N_2) to analyse the gas permeation-separation behaviour (Fig. 3). As described in the experimental part, an α-alumina disc with an optimal surface was used as the substrate in this study, and a γ-alumina-based membrane was also prepared and tested as the reference sample (Fig. S3). It can be seen that both membrane types delivered almost the same gas permeation pattern, indicating again that the 8YSZ sublayer is a perfect substitute for the commonly used γ-alumina layer. Further, we can also see that the gas permeation results are in line with the observed trends in permporometry. Firstly, the smaller but heavier He (kinetic diameter d_k = 0.26 nm) permeated more slowly than the larger and lighter molecule H_2 (d_k = 0.289 nm), which is indicative of Knudsen flow. The measured permeance for He was ~3 10^{-7} mol $m^{-2}s^{-1}Pa^{-1}$. For H_2, the permeance was a factor of ~1.5 higher, which corresponds well to the square root of the ratio of the molar masses, i.e. the theoretical Knudsen permselectivity ($\alpha^*_{He/H2}$=1.4). This confirms that the pores of the membrane were too large to sort the smallest gases, i.e. He and H_2, based on molecular size, as seen in true molecular-sieving amorphous silica membranes [2]. On the other hand, the pore structure appeared sufficiently tight to retard the transport of larger N_2 molecules (d_k = 0.36 nm). As can be seen in Table 1, the permselectivities of He and H_2 achieved with respect to N_2 were 6–7 and 8–11, respectively. These values are considerably higher than the corresponding Knudsen values ($\alpha^*_{He/N2}$=2.6, $\alpha^*_{H2/N2}$=3.7) indicating that gas transport did not only occur via Knudsen flow. However, compared with results reported for some pure silica membranes, the observed selectivity is still quite low. This is attributed to the inherently wider pores of the ethylene-bridged silica used in this work compared to the very dense pure silica material [10]. Also, it was already

seen in permporometry that the membrane contained a fraction of pores with a diameter > 0.4 nm, whereas all test gases have a d_k < 0.4 nm. Nevertheless, the present results suggest that application of the novel 8YSZ/hybrid silica membrane is feasible in, for instance, small gas separation processes that do not require a very high selectivity. While the practical applicability of currently available hybrid silica membranes is limited by the poor stability of the γ-alumina sublayer, the high stability of the 8YSZ sublayer also makes the novel membrane a promising candidate for harsh demanding applications. Although this was not the intention of the present study, measures can also be taken to further improve the small gas selectivity of the membrane, such as decreasing the pore diameter by modification with dopants [e.g. 31,33,34], and making use of a different Si precursor [e.g. 19,29]. For instance, it is very likely that the mesoporous 8YSZ membrane is also perfectly suitable as a platform for other types of hybrid silica membranes, including the BTESM-derived methylene-bridged type, which exhibits a smaller pore diameter and a slightly improved selectivity.

As mentioned in the introduction, an important objective of this work was to investigate the applicability of the novel membrane for CO_2 separation, focusing especially on CO_2 capture from flue gas. Although considerable research has been devoted to the potential of hybrid silica membranes for H_2 separation, applying the membranes for CO_2 separation processes has received rather limited attention so far. This is quite remarkable because adsorption studies on unsupported membranes have shown extensive adsorption of CO_2, even at temperatures > 0°C [e.g. 15,30]. In agreement with these observations, the permeation results of the novel 8YSZ/hybrid silica membrane also indicate clear CO_2-philic permeation behaviour. Referring again to Fig. 3, the CO_2 permeance (~1.5 10^{-7} mol $m^{-2}s^{-1}Pa^{-1}$ [~1.2 $m^3/m^2.h.bar$]) was 4 times higher than that of N_2 at 20°C, and only 3 times lower than that of H_2. For comparison, the corresponding Knudsen values are 0.8 (< 1, because CO_2 is heavier than N_2) and 4.8, respectively. Thus, the permselectivity of CO_2 with respect to N_2 greatly exceeded the value expected for Knudsen diffusion, while the opposite case was found for H_2 and CO_2. We can therefore assume that CO_2 adsorption and surface diffusion occurred and played an important role in gas transport through the membrane. The permeance of CO_2 also decreased with increasing testing temperature, which can also be related to CO_2 adsorption, which becomes weaker at higher temperatures. As H_2 and N_2 did not show this behaviour, the H_2/CO_2 permselectivity increased at higher temperatures – but did not exceed the Knudsen value – while the CO_2/N_2 permselectivity decreased gradually from 4 (20°C) to 2.8 (100°C) and 2 (200°C). Hence, these results suggest that the membrane shows particular potential for CO_2 separation at low temperatures, where the conditions are such that abundant adsorption occurs on the pore walls. In this way, the free space in the pores decreases and the permeation of a non-adsorbing gas, such as N_2, can be effectively blocked, as already shown for zeolite membranes, for example [44].

In order to verify this hypothesis, we conducted a series of permeation tests with three different CO_2/N_2 feed mixtures (50, 15 or 10 vol.% CO_2) at temperatures 20–150°C. The measured CO_2 selectivity and permeance are presented graphically in Figure 4, in panels A and B, respectively. It can be seen that all the membrane samples showed high CO_2/N_2 selectivity at 20°C, with values in the range of 20–30. These values are not only much higher than the ideal Knudsen selectivity (0.8), but are also significantly better than the previously observed single gas permeance ratio of 4, confirming that a selective CO_2 adsorption/pore blocking mechanism occurred. The CO_2 selectivity then visibly decreased with increasing temperature, which may be attributed to a reduced CO_2 adsorption. However, at 50°C this effect was still restricted, and the selectivity remained high in the range of 15–22. Also at higher temperatures, the mixed gas selectivity reached values of 10 (100°C) and 6 (150°C), thus considerably exceeding the single gas permselectivity. It should also be noted that a set of four samples was tested and the CO_2 selectivity plots obtained are nearly the same, thus demonstrating excellent reproducibility for this membrane preparation route. As shown in Fig. 4A, we also investigated the influence of the CO_2 content in the feed mixture and, to our surprise, obtained the same selectivity for each feed composition tested. We can see some scattering in the separation results, but all data points lie more or less closely together. This observation is unusual and counterintuitive, because CO_2 accounted for only 15 or 10 vol.% of the feed mixture in the 2nd and 3rd test series, yet it has important implications for the applicability of the membrane. For example, possible applications are all areas in which a CO_2-philic membrane is required for the removal of CO_2 from a diluted gas mixture. Importantly, this implies that the membrane also has the required characteristics for postcombustion CO_2 capture from flue gas, which typically contains 10–15% CO_2, the rest being mainly N_2. In addition, we speculate that the

membrane is equally useful for other important CO_2 separation applications, such as CO_2 removal from natural gas, CO_2 recovery from landfill gas and CO_2 capture and utilization in heavy industries (e.g. cement, iron, steel).

For practical application in a power plant, a candidate membrane should also fulfil two other important requirements: stability in the exhaust gas of the power plant and ability to permeate a large volume of CO_2. Given the low CO_2 content in flue gas and the quasi-atmospheric pressure conditions in the flue gas duct of power plants, the need for high CO_2 permeance is obvious. According to Xomeritakis *et al.* [7], the level required for large-scale application in a power plant is > 2 MPU, where 1 MPU = 10^{-7} mol $m^{-2}s^{-1}Pa^{-1}$ or ~0.8 m^3/m^2.h.bar. Merkel *et al.* [50] indicated that membranes need to have a minimum CO_2 permeance of about 1000 GPU and CO_2/N_2 selectivity of greater than 20 to make CO_2 capture with membranes economically feasible, where 1000 GPU = 3.35 10^{-7} mol $m^{-2}s^{-1}Pa^{-1}$ or 2.7 m^3/m^2.h.bar. In Figure 4B, the CO_2 permeance data corresponding to the separation results given in panel A are plotted. As can be seen, there is considerable scattering in the results and the permeance data show relatively little coherence. However, a clear increasing or decreasing trend as a function of testing temperature or feed composition cannot be recognized. In principle, the broad variation in the CO_2 permeance values is not a problem, because all the tested samples display values in a range between ~1 to 4 $m^3/(m^2hbar)$, which approaches the level necessary for practical application. Most importantly, it is demonstrated here that the membrane is able to separate sufficient volumes of CO_2 from a diluted gas mixture with N_2 and that it is particularly selective at lower temperatures < 50°C, which are the typical conditions in the flue gas duct. Moreover, it should be emphasized again that the membrane also has excellent prospects for the humid and harsh conditions that are encountered in the power plant. This was verified by performance and stability tests in a real power plant, where 8YSZ-based sublayers were successfully tested. In contrast, reference samples that contained conventional γ-alumina layers failed in the same test set-up [51].

In order to obtain an impression of the performance of the novel 8YSZ/hybrid silica membrane in pervaporation, we first screened a series of identically prepared samples, 105 mm and 250 mm in length, at 70°C with a 5 wt.% water and 95 wt.% isopropanol (IPA) feed mixture. As can be seen in Table 2, all the tested samples exhibited selective permeation of water (d_k = 0.26 nm) and the larger IPA molecules (d_k = 0.48 nm) were mostly excluded. The measured water/IPA selectivity was very high, with values fluctuating between 140 to 716. It thus appeared that the membrane, which possessed a few defective areas in SEM, exhibited outstanding separation behaviour. Meanwhile, the fluxes were also observed to be very good, reaching values between 4.5 and 6.4 kg $m^{-2}h^{-1}$. These extraordinary values indicate that water molecules permeate very rapidly through the entire membrane system, which is thought to be due to the graded architecture of the 8YSZ sublayer, comprising a thicker and more open layer with ~5–6 nm pores and a much thinner and more compact layer with ~3–4 nm pores. In contrast, the γ-alumina sublayer of a conventional hybrid silica membrane exhibits a uniform structure with ~3 nm pores across the entire membrane layer. It is important to note that an extensive set of ten samples was tested here and, disregarding some scattering in the water/IPA selectivity, the obtained results are very similar, demonstrating again excellent reproducibility of the manufacturing methods. In Table 2, membranes prepared on shorter 105 and longer 250 mm tubes are compared, and some samples were also thermally treated at 450°C instead of 300°C. These different manufacturing parameters did not, however, result in great differences in overall membrane performance.

Encouraged by the excellent results from these preliminary tests, a set of four 250 mm tubes was further examined at three different temperatures (70, 100, 140°C) with three different 5 wt.% water/alcohol mixtures (EtOH, IPA, n-BuOH). The separation and flux data obtained are displayed in panels A and B of Figure 5. As expected, all the tested samples showed high water/IPA and water/BuOH selectivity at 70°C, with values ranging from ~250 to 600 and accompanying fluxes of ~5 kg $m^{-2}h^{-1}$. After increasing the operating temperature to 100°C, the flux was found to increase to ~10 kg $m^{-2}h^{-1}$, which is an extremely high value. Meanwhile, all the samples delivered a somewhat lower water selectivity, but the achieved values were still very good and fluctuated between 150 and 450. At 140°C, the flux increased further to values above 15 kg $m^{-2}h^{-1}$, while only little selectivity degradation was observed. To the best of our knowledge, these results are among the best ever obtained for a membrane with an industrially relevant shape, and they compare very well to the benchmark results of Castricum *et al.* , Kreiter *et al.* and van Veen *et al.*. On the other hand, experiments with water/EtOH mixtures were not successful. Obviously, the pores in the membrane were too large to sieve out EtOH molecules (d_k = 0.35 nm), but

were sufficiently small to inhibit the permeance of IPA (d_k = 0.48 nm) and BuOH (d_k = 0.55 nm). Possibly, the application of a methylene-bridged silica, as described by Kreiter et al. [19] and Kanezashi et al. [29], could lead to an ethanol-selective 8YSZ-supported membrane.

4. Conclusion

In conclusion, a next-generation hybrid silica membrane with great potential for CO_2 separation and water pervaporation was successfully produced. The unique feature of this membrane is that it is prepared on a mesoporous yttria-stabilized (8YSZ) membrane instead of the commonly used but unstable γ-alumina membrane. As such, a huge improvement in material stability is achieved. With respect to applications, the novel membrane has characteristics that are of interest for CO_2 capture from a power plant flue gas stream, including adequate permeance, CO_2/N_2 selectivity and tolerance to water vapour. In addition, we speculate that the membrane could also be used for other important and challenging CO_2 separation applications. In the field of pervaporation, all of the areas where microporous membranes are currently considered for the dehydration of higher alcohols, including propanol and butanol, also represent possibilities. More research is needed here to identify and evaluate further exciting and challenging applications, e.g. the dehydration of organic acids. Importantly, any large-scale application of a novel membrane requires methods to fabricate large areas of membranes on a technical-grade support material in a cost-effective way. In the present work, all membrane layers were prepared by dip coating, a technology that is mature, scalable and widely practised in the manufacturing of porous ceramic membranes. The membranes were also reproducibly prepared on regular macroporous α-alumina supports and in this respect no scale-up difficulties can be foreseen. However, before the membranes can be employed in practical applications, their long-term stability in the respective applications must be further investigated.

Acknowledgements

The contribution of the following colleagues is greatly acknowledged: Dr. Doris Sebold (SEM) and Lars Petter (CO_2/N_2 mixed gas permeation tests). Han Heuver (PERVATECH BV, the Netherlands) is also gratefully acknowledged for performing the pervaporation tests.

References

[1] R.M. de Vos, H. Verweij, High selectivity, high flux silica membranes for gas separation, Science 279 (1998) 1710-11

[2] S.T. Oyama, D. Lee, P. Hacarlioglu, R.F. Saraf, Theory of hydrogen permeability in nonporous silica membranes, J. Membr. Sci. 244 (2004) 45-53

[3] F.P. Cuperus, R.W. van Gemert, Dehydration using ceramic silica pervaporation membranes – the influence of hydrodynamic conditions, Sep. Purif. Technol. 27 (2002) 225-229

[4] T.A. Peters, J. Fontalvo, M.A.G. Vorstman, N.E. Benes, R.A. Van Dam, Z.A.E.P. Vroon, E.L.J. van Soest-Vercammen, J.T.F. Keurentjes, Hollow fibre microporous silica membranes for gas separation and pervaporation: synthesis, performance and stability, J. Membr. Sci. 248 (2005) 73-80

[5] G. Xomeritakis, C.-Y. Tsai, C.J. Brinker, Microporous sol–gel derived aminosilicate membrane for enhanced carbon dioxide separation, Sep. Purif. Technol. 42 (2005) 249-257

[6] G. Xomeritakis, N.G. Liu, Z. Chen, Y.-B. Jiang, R.Köhn, P.E. Johnson, C.-Y. Tsai, P.B. Shah, S. Khalil, S. Singh, C.J. Brinker, Anodic alumina supported dual-layer microporous silica membranes, J. Membr. Sci. 287 (2007) 157-161

[7] G. Xomeritakis, C.Y. Tsai, Y.B. Jiang, C.J. Brinker, Tubular ceramic-supported sol–gel silica-based membranes for flue gas carbon dioxide capture and sequestration, J. Membr. Sci. 341 (2009) 30–36

[8] A. Nijmeijer, H. Kruidhof, R. Bredesen, H. Verweij, Preparation and properties of hydrothermally stable γ-alumina membranes, J. Am. Ceram. Soc. 84 (2001) 136-140

[9] (a) H. Verweij, Inorganic membranes, Current Opinion in Chemical Engineering 1 (2012) 1-7; (b) H. Verweij, Y.S. Lin, J. Dong, Microporous Silica and Zeolite Membranes for Hydrogen Purification, MRS Bulletin 31 (2006) 756-764

[10] J.E. ten Elshof, Hybrid materials for molecular sieves, Handbook of Sol-Gel Science and Technology, L. Klein et al. (eds.), Springer International Publishing Switzerland 2016, p. 1-27
[11] H.L. Castricum, R. Kreiter, H.M. van Veen, D.H.A. Blank, J.F. Vente, J.E. ten Elshof, High performance hybrid pervaporation membranes with superior hydrothermal and acid stability. J. Membr. Sci. 324 (2008) 111-118
[12] H.L. Castricum, A. Sah, R. Kreiter, D.H.A. Blank, J.F. Vente, J.E. ten Elshof, Hydrothermally stable molecular separation membranes from organically linked silica, J. Mater. Chem. 2008 (18) 2150-2158
[13] H.L. Castricum, A. Sah, J.A.J. Geenevasen, R. Kreiter, D.H.A. Blank, J.F. Vente, Structure of hybrid organic-inorganic sols for the preparation of hydrothermally stable membranes, J Sol-Gel Sci. Technol. 48 (2008) 11-17
[14] H.L. Castricum, A. Sah, R. Kreiter, D.H.A. Blank, J.F. Vente, J.E. ten Elshof, Hybrid ceramic nanosieves: stabilizing nanopores with organic links. Chem. Commun. 9 (2008) 1103-1105
[15] H.L. Castricum, G.G. Paradis, M.C. Mittelmeijer-Hazeleger, R. Kreiter, J.F. Vente, J.E. ten Elshof, Tailoring the separation behavior of hybrid organosilica membranes by adjusting the structure of the organic bridging group, Adv. Funct. Mater. 21 (2011) 2319-2329
[16] H.L. Castricum, G.G. Paradis, M.C. Mittelmeijer-Hazeleger, W. Bras, G. Eeckhaut, J.F. Vente, Tuning the nanopore structure and separation behavior of hybrid organosilica membranes, Microporous Mesoporous Mater. 185 (2014) 224-234
[17] H.L. Castricum, H.F. Qureshi, A. Nijmeijer, L. Winnubst, Hybrid silica membranes with enhanced hydrogen and CO_2 separation properties, J Membr Sci. 488 (2015) 121-128
[18] R. Kreiter, M.D.A. Rietkerk, H.L. Castricum, H.M. van Veen, J.E. ten Elshof, J.F. Vente, Stable hybrid silica nanosieve membranes for dehydration of lower alcohols, Chem.Sus.Chem. 2 (2009) 158-160
[19] R. Kreiter, M.D.A. Rietkerk, H.L. Castricum, H.M. van Veen, J.E. ten Elshof, J.F. Vente, Evaluation of hybrid silica sols for stable microporous membranes using high-throughput screening, J Sol-Gel Sci Technol 57 (2011) 245-252
[20] H.M. van Veen, M.D.A. Rietkerk, D.P. Shanahan, M.M.A. van Tuela, R. Kreiter, H.L. Castricum, J.E. ten Elshof, J.F. Vente, Pushing membrane stability boundaries with HybSi® pervaporation membranes, J. Membr. Sci. 380 (2011) 124-131
[21] https://www.hybsi.com/
[22] R.J.R. Uhlhorn, M.H.B.J. Huis in 't Veld, K. Keizer, A.J. Burggraaf, Synthesis of ceramic membranes, Part I Synthesis of non-supported and supported γ-alumina membranes without defects, J. Mater. Sci. 27 (1992) 527-537
[23] R.J.R. Uhlhorn, K. Keizer, A.J. Burggraaf, Gas transport and separation with ceramic membranes. Part II. Synthesis and separation properties of microporous membranes, J. Membr. Sci. 66 (1992) 271-287
[24] R.S.A. de Lange, J.H.A. Hekkink, K. Keizer, A.J. Burggraaf, Permeation and separation studies on microporous sol–gel modified ceramic membranes, Microporous Mater. 4 (1995) 169-86
[25] A. Sah, Chemically modified ceramic membranes – Study of structural and transport properties, PhD Thesis, UTwente, the Netherlands, 2006
[26] A. Sah, H.L. Castricum, J.F. Vente, D.H.A. Blank, J.E. ten Elshof, Microporous molecular separation membrane with high hydrothermal stability, WO/2007/081212
[27] M. Kanezashi, K. Yada, T. Yoshioka, T. Tsuru, Design of silica networks for development of highly permeable hydrogen separation membranes with hydrothermal stability, J. Am. Chem. Soc. 131 (2009) 414-415
[28] M. Kanezashi, K. Yada, T. Yoshioka, T. Tsuru, Organic–inorganic hybrid silica membranes with controlled silica network size: preparation and gas permeation characteristics, J. Membr. Sci. 348 (2010) 310-318
[29] M. Kanezashi, M. Kawano, T. Yoshioka, T. Tsuru, Organic-inorganic hybrid silica membranes with controlled silica network size for propylene/propane separation, Ind Eng Chem Res. 51 (2012) 944-953
[30] H. Qi, J. Han, N.P. Xu, H.J.M. Bouwmeester, Hybrid organic-inorganic microporous membranes with high hydrothermal stability for the separation of carbon dioxide, Chem.Sus.Chem., 2010, 3(12), 1375-1378.
[31] H. Qi, H. Chen, L. Li, G. Zhu, N. Xu, Effect of Nb content on hydrothermal stability of a novel ethylenebridged silsesquioxane molecular sieve membrane for H_2/CO_2 separation, J. Membr. Sci. 421 (2012) 190-200
[32] T. Tsuru, T. Shibata, J.H. Wang, H.R. Lee, M. Kanezashi, T. Yoshioka, Pervaporation of acetic acid aqueous solutions by organosilica membranes, J. Membr. Sci. 421 (2012) 25-31
[33] M.J. Wolf, E.J. Kappert, J.T.G. te Braake, A. Nijmeijer, S. Roitsch, J. Mayer, H.J.M. Bouwmeester, Thermal stability and gas separation performance of hybrid inorganic-organic silica membranes, https://www.researchgate.net/publication/295688683_Thermal_stability_and_gas_separation_performance_of_hybrid_inorganic-organic_silica_membranes
[34] M. ten Hove, A. Nijmijer, L. Winnubst, Facile synthesis of zirconia doped hybrid organic inorganic silica membranes, Sep. Purif. Technol. 147 (2015) 372-378
[35] https://www.atech-innovations.com/home.html

[36] https://www.inopor.com/en/

[37] http://www.tami-industries.com/technology/ceramic-membranes/

[38] https://www.alsys-group.com/en/ceramic-membranes/

[39] R. Vacassy, C. Guizard, V. Thoraval, L. Cot, Synthesis and characterisation of microporous zirconia powders. Application in nanofiltration characteristics, J. Membr. Sci. 132 (1997) 109-118

[40] P. Puhlfürß, A. Voigt, R. Weber, M. Morbé, Microporous TiO2 membranes with a cut-off <500 Da, J. Membr. Sci. 174 (2000) 123-133

[41] J. Sekulic, J.E. ten Elshof, D.H.A. Blank, A microporous titania membrane for nanofiltration and pervaporation, Adv. Mat. 72 (2004) 49-57

[42] T. Van Gestel, J. Barthel, New types of graphene-based membranes with molecular sieve properties for He, H_2 and H_2O, J. Membr. Sci. 554 (2018) 378-384

[43] T. Van Gestel, D. Sebold, Hydrothermally stable mesoporous ZrO_2 membranes prepared by a facile nanoparticle deposition process, Sep. Purif. Technol. 221 (2019) 399-407

[44] M.P. Bernal, J. Coronas, M. Menendez, J. Santamarıa, Separation of CO_2/N_2 mixtures using MFI-Type Zeolite membranes, AIChE Journal 50 (2004) 127-135

[45] H. Richter, H. Voss, N. Kaltenborn, S. Kämnitz, A. Wollbrink, A. Feldhoff, J. Caro, S. Roitsch, I. Voigt, High-flux carbon molecular sieve membranes for gas separation, Angew. Chem. Int. Ed. 56 (2017) 7760 -7763

[46] a) F.P. Cuperus, C.A. Smolders, Characterization of UF membranes, Membrane characteristics and characterization techniques. Adv. Colloid Interface Sci. 34 (1991) 135. b) F.P. Cuperus, D. Bargeman, C.A. Smolders, Permporometry. The determination of the size distribution of active pores in UF membranes, J. Membr. Sci. 71 (1992) 57-67

[47] G.Z. Cao, J. Meijernik, H.W. Brinkman, A.J. Burggraaf, Permporometry study on the size distribution of active pores in porous ceramic membranes, J. Membr. Sci. 83 (1993) 221-235.

[48] T. Tsuru, T. Hino, T. Yoshioka, M. Asaeda, Permporometry characterization of microporous ceramic membranes, J. Membr. Sci. 186 (2001) 257-265.

[49] S. Zeidler, P. Puhlfürß, U. Kätzel, I. Voigt, Preparation and characterization of new low MWCO ceramic nanofiltration membranes for organic solvents, J Membr. Sci. 470 (2014) 421-430

[50] T. Merkel, K. Amo, R. Baker, R. Daniels, B. Firat, Z. He, H. Lin, A. Serbanescu, X. Wei, H. Wijmans, Membrane process to sequester CO_2 from power plant flue gas, Technical report, July 2009, https://www.osti.gov/servlets/purl/1015458-INdTMC/

[51] J. Eiberger, K. Wilkner, C. Reetz, D. Sebold, N. Jordan, M. de Graaff, W.A. Meulenberg, D. Stöver, M. Bram, Influence of coal power plant exhaust gas on the structure and performance of ceramic nanostructured gas separation membranes, International journal of greenhouse gas control 43 (2015) 46-56

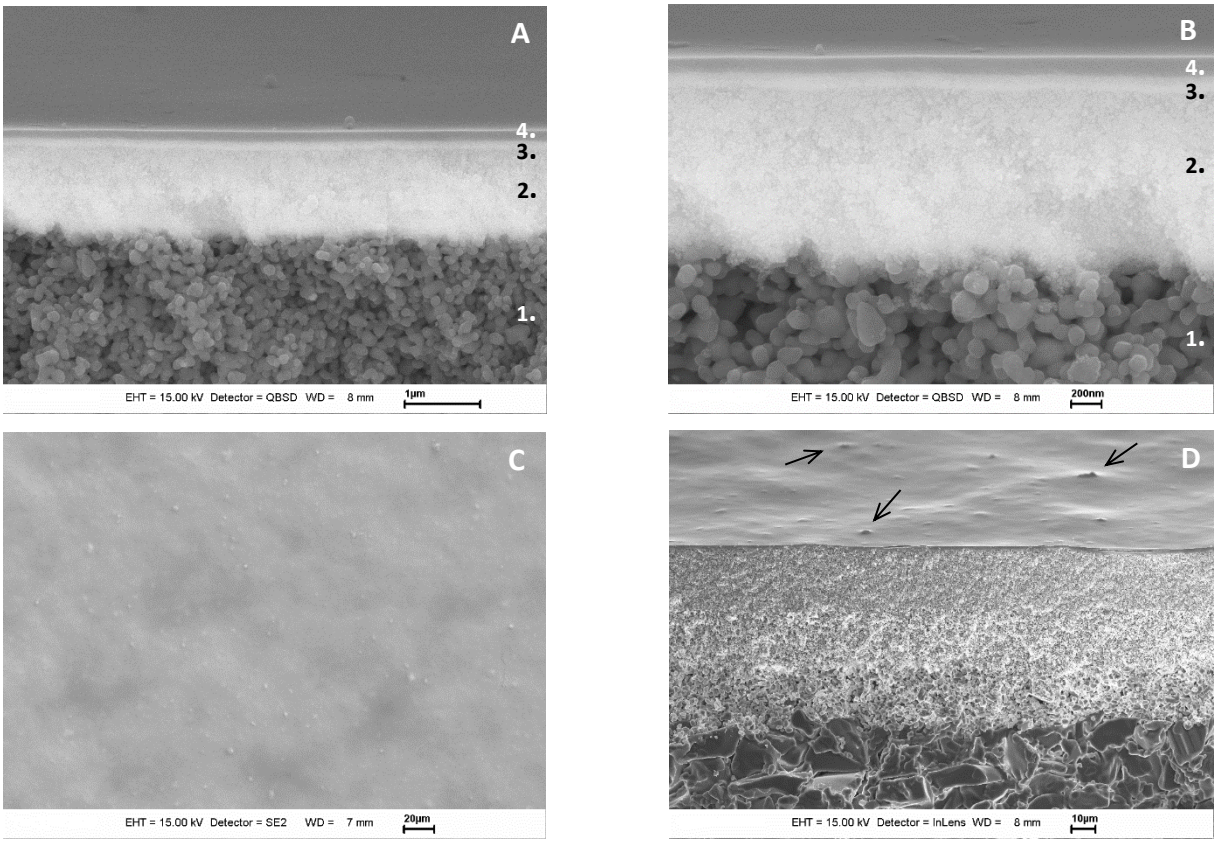

Figure 1. Composite membrane, comprising 8YSZ mesoporous layers and hybrid silica top layer. Field-emission scanning electron microscopy (FE-SEM) images of a membrane on a tubular macroporous α-alumina support produced by dip coating. The upper panels show the cross-section in the back-scattering mode (**A**), and a detail of this image (**B**). The lower panels show the surface in a 2-D view (**C**) and in an angled, 3-D perspective view (**D**). [Panel (**A** + **B**): **1.** α-alumina support, **2.** two mesoporous 8YSZ layers with a pore size of ~5–6 nm, **3.** two mesoporous 8YSZ layers with a pore size of ~3–4 nm, **4.** two hybrid silica top layers]

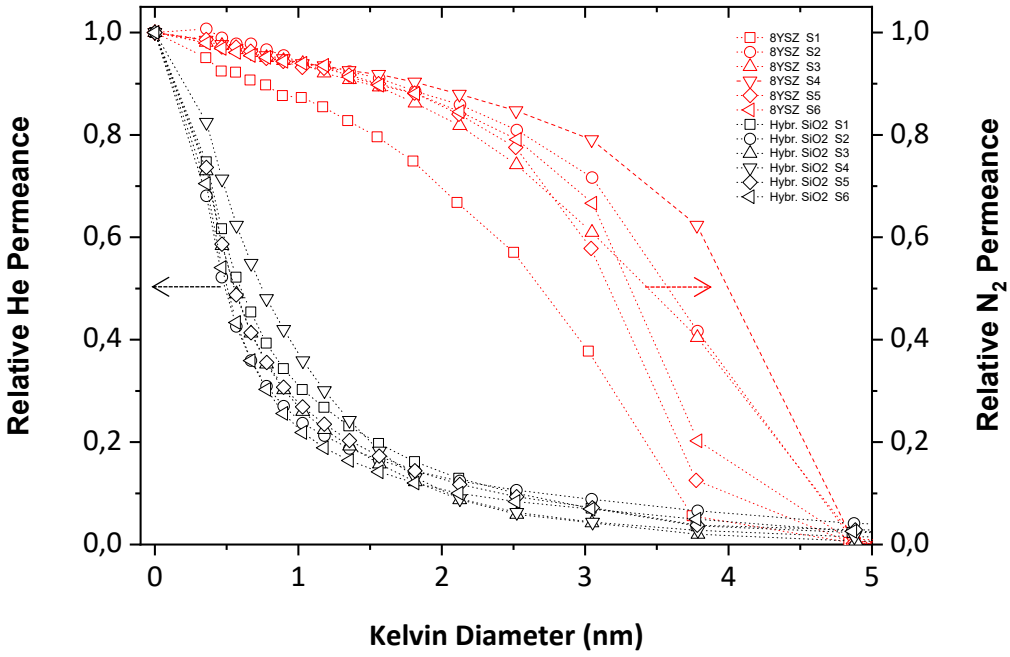

Figure 2. He permeance through a hybrid silica membrane supported on mesoporous 8YSZ, as measured by permporometry. The black data points indicate the results obtained for the hybrid silica-coated membrane system. The red data points indicate results obtained for the corresponding mesoporous 8YSZ layers, measured with N_2 as carrier gas. The data points were obtained for six identically prepared tubular samples (S1, S2, S3, … , S6).

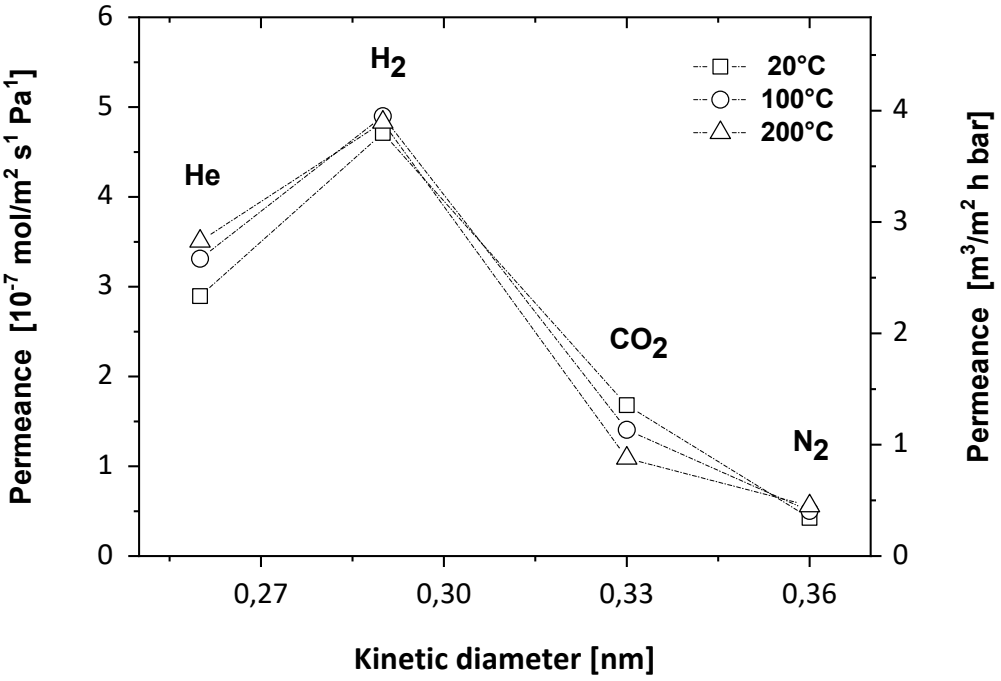

Figure 3. Single-gas permeation through a hybrid silica membrane supported on mesporous 8YSZ. Permeances of gases with a kinetic diameter of 0.26 nm to 0.36 nm at different temperatures. The data points were obtained with a disc shaped sample (diameter 40 mm).

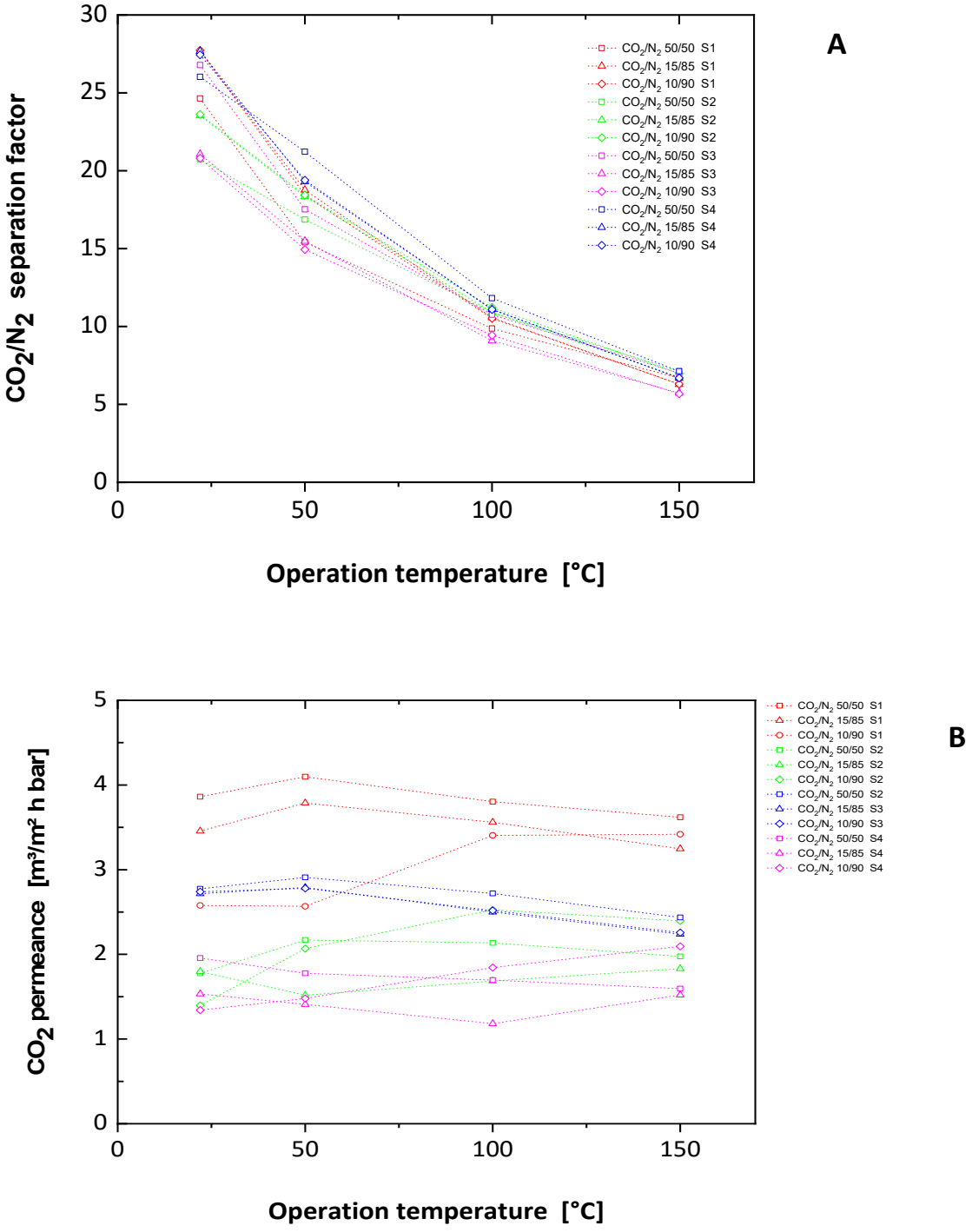

Figure 4. CO_2/N_2 gas mixture separation. CO_2/N_2 separation factor (**A**) and CO_2 permeation flux (**B**) as a function of temperature for several feed compositions (50, 15 or 10 vol.% CO_2). The data points indicate the results obtained for a series of four identically prepared tubular 250 mm samples (S1, S2, S3, S4).

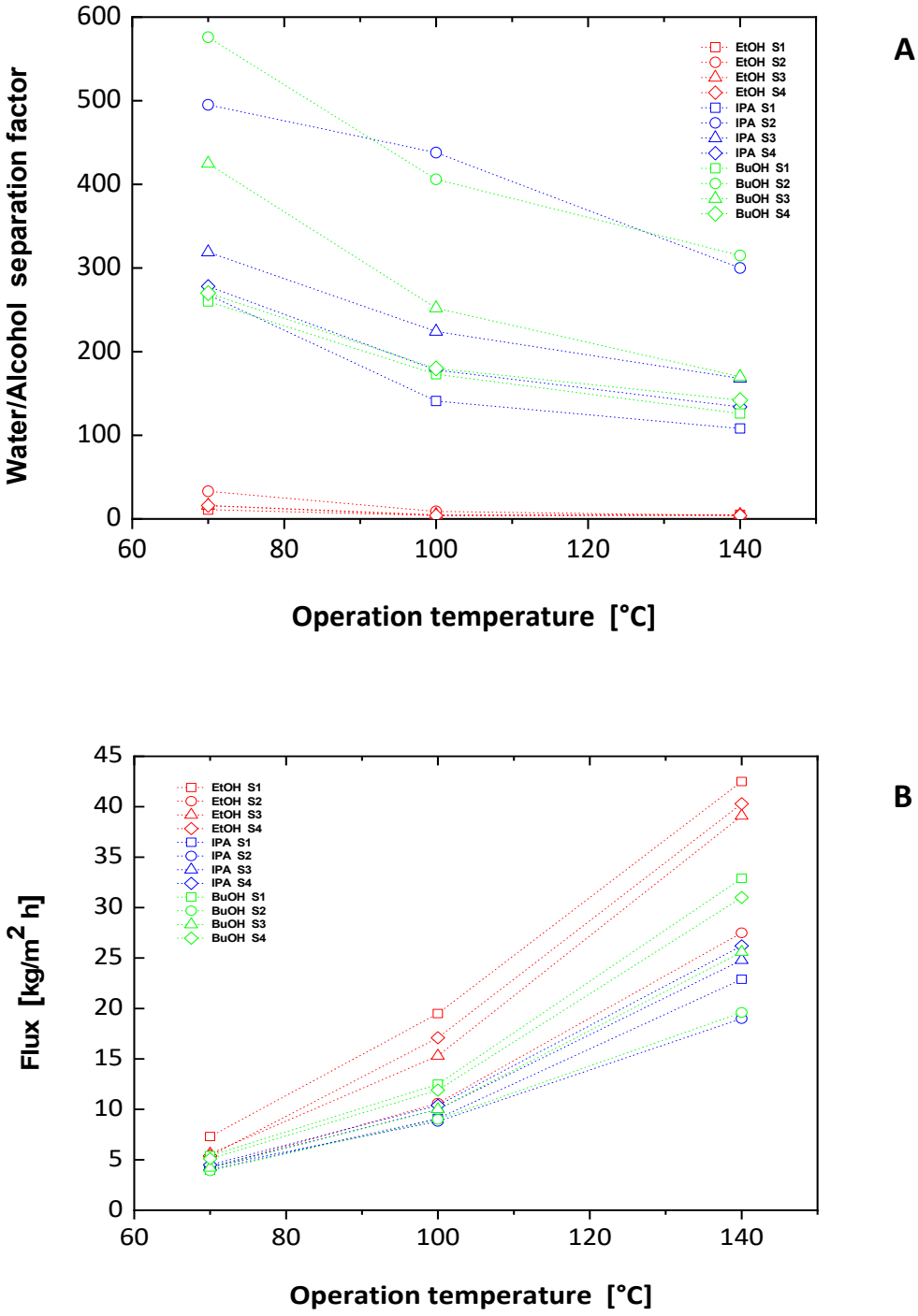

Figure 5. Water/alcohol pervaporation. Water separation factor (**A**) and total permeation flux (**B**) as a function of temperature for several feed solutions containing 5 wt.% water and 95 wt.% ethanol (EtOH), isopropanol (IPA) or n-butanol (BuOH). The data points indicate the results obtained for a series of four identically prepared tubular 250 mm samples (S1, S2, S3, S4).

Table 1. Single-gas permeation through a hybrid silica membrane supported on mesporous 8YSZ. Permselectivity of relevant gas pairs with a kinetic diameter of 0.26 nm to 0.36 nm and at different temperatures.

	He/N_2	**H_2/N_2**	**H_2/CO_2**	**CO_2/N_2**
20°C	6.8	8.6	2.8	4
100°C	6.6	9.7	3.5	2.8
200°C	6.2	11	4.4	2

Table 2. Results of pervaporation screening tests at 70°C with a feed solution containing 5 wt.% water and 95 wt.% isopropanol (IPA). The results were obtained for a series of ten tubular samples with a length of 105 and 250 mm.

Sample Nr.	Tube length	Thermal treatment	Flux @ 70°C	Water/IPA
1	105 mm	450°C vacuum	6.4	523
2	105 mm	450°C vacuum	6.1	153
3	105 mm	450°C vacuum	4.5	474
4	105 mm	300°C vacuum	5.3	716
5	105 mm	300°C vacuum	5.8	140
6	105 mm	300°C vacuum	6.1	277
7	250 mm	300°C vacuum	5.9	209
8	250 mm	300°C vacuum	4.9	286
9	250 mm	300°C vacuum	5.2	334
10	250 mm	300°C vacuum	5.4	208

Supplementary Information

Fig. S1. **Image of the dip-coating equipment.** The reservoir with the coating liquid is moved up and down, while the support to be coated remains in the same position.

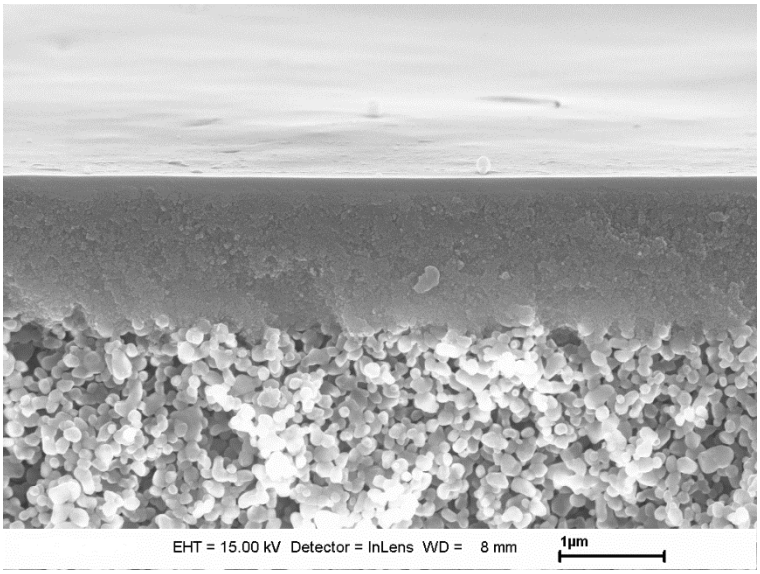

Figure S2. Composite membrane, comprising 8YSZ mesoporous layers and hybrid silica top layer. Field-emission scanning electron microscopy (FE-SEM) image of a membrane on a tubular macroporous α-alumina support produced by dip-coating. The image shows the cross-section in the in-lens mode.

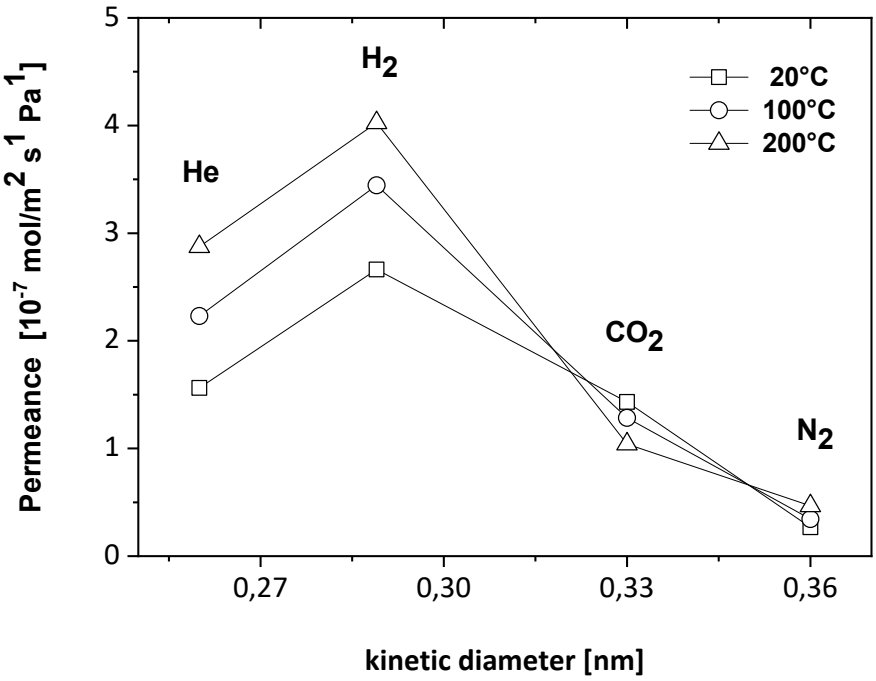

Figure S3. Single-gas permeation through a hybrid silica membrane supported on mesporous γ-alumina. Permeances of gases with a kinetic diameter of 0.26 nm to 0.36 nm at different temperatures. The data points were obtained with a disc shaped sample (diameter 40 mm).

Table S1. Single-gas permeation through a hybrid silica membrane supported on mesporous γ-alumina. Permselectivity of relevant gas pairs with kinetic diameters of 0.26 nm to 0.36 nm and at different temperatures.

	He/N_2	**H_2/N_2**	**H_2/CO_2**	**CO_2/N_2**
20°C	6	10	2	5.5
100°C	6	10	2.6	3.7
200°C	6.2	8.6	3.9	2